

**INLET FOGGING OF GAS TURBINE ENGINES – EXPERIMENTAL AND ANALYTICAL INVESTIGATIONS
 ON IMPACTION PIN FOG NOZZLE BEHAVIOR**

Mustapha A. Chaker, Ph. D.
 Director, Research and Development

Cyrus B. Meher-Homji, P.E.
 Chief Engineer

Thomas Mee III
 Chairman and CEO

Mee Industries Inc., Gas Turbine Division
 Monrovia, California, USA

T_a Temperature of air (C)

ABSTRACT

The inlet fogging of gas turbine engines for power augmentation has seen increasing application over the past decade. This paper provides the results of extensive experimental and theoretical studies conducted on impaction pin fog nozzles. It covers the important area of the fog plume pattern of impaction pin nozzles and examines fog-plume uniformity. The subject of sprinkle (large droplet formation) from the nozzles is also examined in detail and is shown to be non-significant. The effect, on evaporation rate, of ambient climatic conditions and the location of the fog nozzle with respect to the gas turbine inlet duct has been analytically and experimentally analyzed. An Analytical model is used to study the evaporation dynamics of fog droplets injected in the inlet ducts the model is validated experimentally in a wind tunnel.

T_d Droplet Temperature (C)
 V_{rel} Droplet relative velocity (m.s⁻¹)
 We Weber number

GREEK ALPHABET

λ_a Thermal conductivity, air (W.m⁻¹. C⁻¹)
 μ_a Dynamic viscosity, air (kg.m⁻¹.s⁻¹)
 ρ_a Density, air (kg.m⁻³)
 γ_w Water Surface tension (N.m⁻¹)
 η_{ev} Evaporation Efficiency (%)
 ΔT Temperature Difference (C)

NOMENCLATURE

C_{p_a} Specific heat of air (J.kg⁻¹. C⁻¹)
 C_{p_d} Specific heat of water (J.kg⁻¹. C⁻¹)
 D_{32} Sauter mean diameter (microns)
 D_d Droplet diameter (microns)
 Df_a Mass coefficient of diffusion for air (m².s⁻¹)
 Df_{mass} Coefficient of mass diffusion (m.s⁻¹)
 Dv_{90} is a diameter for which 90% of the water volume in the spray is less than or equal to (microns)
 h_{cv} Coefficient of thermal convective exchange (W.m⁻¹. C⁻¹)
 I Iteration in the evaporation dynamics model
 L_v Latent heat of vaporization of water (J.Kg⁻¹)
 P_a Atmospheric pressure (Pa)
 P_{v_w} Vapor pressure at the interface droplet-air (Pa)
 RA Active Radius (microns)
 RH Relative Humidity (%)
 S_d Droplet surface (m²)

SUBSCRIPT

a air
 d droplet
 t time
 i initial

1. INTRODUCTION AND BACKGROUND

Gas Turbine output is significantly impacted by the temperature of the ambient air, with power output dropping by 0.54% to 0.90% for every 1 C (1.8°F) rise in ambient temperature. This loss in output presents a significant problem to utilities, cogenerators and merchant power plants, particularly when electric demands are high during the hot months. Inlet fogging is a popular technique for boosting the hot-weather performance of gas turbines and has been extensively implemented over the past decade. Inlet fogging fits the niche of low-cost power augmentation and has consequently become very popular.

The concept is a simple one in which a direct evaporation effect is derived by the use of fog generated by high-pressure pumps and atomizing nozzles installed in the inlet duct downstream of the inlet air filters. The fog evaporates in the inlet duct and cools the air down to the wet bulb temperature.

It is estimated that more than 700 gas turbines have been fitted with fogging systems including many modern class F gas turbines. In spite of this proliferation of inlet fogging systems, there is not much technical literature available covering the thermodynamics, physics and engineering principles that govern the fogging process. The first rigorous and detailed treatment was made by Chaker et al [1, 2, 3] and this paper builds on that foundation.

Fog intercooling¹, which has been applied from the early days of gas turbine and jet engine technology is a technique that consists of spraying more fog than will evaporate under the given ambient temperature and humidity conditions so that non-evaporated liquid water droplets enter the compressor. The desired quantum of un-evaporated fog is carried with the air stream into the compressor where it evaporates and produces an intercooling effect. The resulting reduction in the work of compression can give a significant additional power boost and an improved heat rate.

A review of the basic principles of fogging technology can be found in Meher-Homji and Mee [4,5]. Early papers on fog intercooling and wet compression started to appear in the late 1940s including Kleinschmidt² [6], and Wilcox & Trout [7]. Other references include Hill [8], Arsen'ev and Berkovich [9], Nolan and Twombly³ [10] and Utamura et al [11].

Most inlet fogging systems currently in operation employ one of two different types of fogging nozzles; swirl jet nozzles or impaction pin nozzles. This paper studies the behavior of impaction pin nozzles designed by Mee Industries as shown in **Figure 1** and gives some commentary on swirl jet type nozzles as well. There are several misconceptions regarding the behavior of impaction pin nozzles and this paper makes a systematic study of several of them.

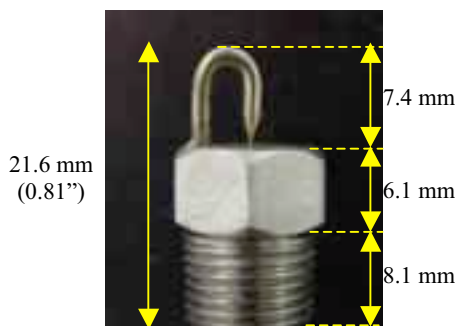


Figure 1. Impaction Pin Nozzle

Topics covered in this paper include:

Effects of airflow velocity and ambient Relative Humidity on droplet size. Fogging systems have to operate at varying humidity conditions but, at this time, there has been no

published systematic study of the effect of ambient conditions on fogging system performance.

Effects of fog plume shape and non-uniformity caused by displacement of the impaction pin: In this paper we have made detailed measurements of the effect of partial pin displacement on droplet size and examined the behavior of the droplets in multiple locations in the spray plume. A discussion is also made of the forces required for movement of the impaction pin.

Large droplet formation: A systematic study has been done of what we call the *sprinkle effect*. This effect can occur when the spray plume strikes the support side of the impaction pin. Water can accumulate on the pin and form large droplets, which are then stripped off and enter the airflow. The research presented here shows that the sprinkle effect occurs, with Mee impaction pin nozzles, only at lower than normal operating pressures and that sprinkle occurs with both swirl jet and impaction pin nozzles. But in both cases it has an insignificant effect on the performance of the fogging system or on the compressor blades.

Heat and mass transfer model: A detailed droplet heat and mass transfer model was developed by Chaker [1] and is extended in this paper to include application to the whole range of droplets found in a typical inlet fogging spray. The results are provided for a range of ambient psychrometric conditions and graphical results are provided to assist gas turbine users in understanding the significance of droplet size on fog system performance. This model allows the calculation of evaporative efficiency and predicts the size of non-evaporated droplets that may enter the compressor. It also quantifies the reduction in evaporative efficiency that naturally occurs with an increase in ambient relative humidity. While this phenomenon is intuitively clear, the model and curves provide greater insight and a means for making practical calculations.

Effects of fog nozzle location on fog system performance: The position of the nozzle array in the inlet duct is an important design consideration as it affects both the size of the initial droplet (due to the effect of airflow) and the residence time for the droplets in the duct prior to reaching the compressor. This subject is discussed in detail including an example of a typical installation.

2. EXPERIMENTAL SETUP

In order to measure droplet sizes in conditions similar to those found in gas turbine inlet ducts, a variable speed wind tunnel was used, as shown in **Figure 2**. A brief description of the wind tunnel is given below and more information regarding its configuration and instrumentation may be found in Chaker [1,3]. Fog is generated in the wind tunnel by forcing high-pressure, filtered and deionized water through the small orifice nozzles. In the experimental setup, a variable-speed-drive, positive-displacement, ceramic-plunger pump is used to generate water pressures up to 207 bar (3000 psi).

Droplet size measurement was done with nozzles located in the constricted section of the duct, where the highest airflow velocities are attainable. Measurements were taken at different locations in the spray plume using a Malvern Spraytec RTS5114 laser particle analyzer, as shown in **Figure 3**. The Malvern system is based on a laser diffraction technique [12]. This is a spatial sampling system; consequently it allows the sampling of a large number of droplets instantaneously with a frequency up to 2500 Hz.

¹ Also known as overspray or wet compression.

² This paper coined the term "wet compression".

³ Nolan and Twombly covered an application of fog intercooling on GE Frame 5 engines.



Figure 2. Experimental wind tunnel, 10.5m (34.5 ft.) long and capable of velocities up to 25 m/sec (4900 ft/min). Used to study droplet kinetics and thermodynamics under conditions similar to gas turbine inlet air ducts.

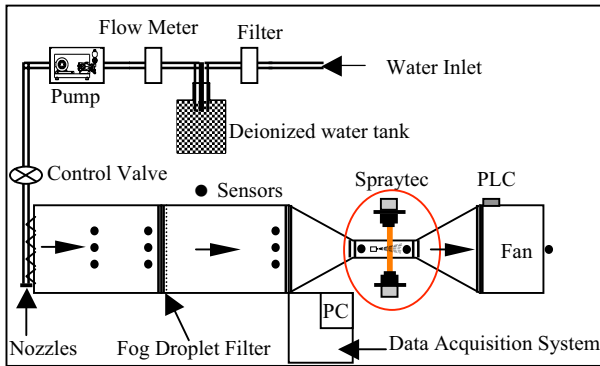


Figure 3. Wind Tunnel experimental setup

A nozzle manifold, installed at the inlet of the duct, was turned off when measurements were taken at ambient conditions. For measurements with a saturated airflow these nozzles were turned on, **Figure 4**, and a fog droplet filter was used, as shown in **Figure 3**, to remove any un-evaporated droplets.



Figure 4. Fog nozzles manifold used to create saturated air in the wind tunnel. The use of a fog droplet filter makes it possible to achieve an airflow with very close to 100% RH.

Droplet size measurements, as shown in **Figure 5**, were taken in the constricted portion of the wind tunnel, at different locations in the spray plume and at different airflow velocities.

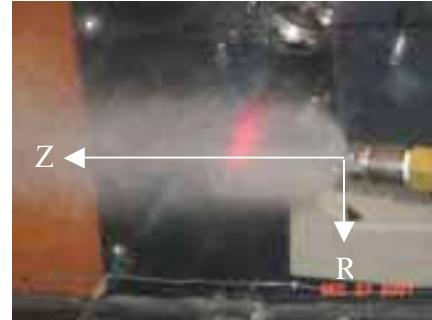


Figure 5. Droplet size measurement in the wind tunnel

3. EFFECT OF AIR VELOCITY AND HUMIDITY ON DROPLET SIZE

It is important to understand the effects of airflow velocity and humidity on the atomization process because the nozzle manifolds can be installed at different locations in the inlet duct (with differing air velocities) and fog systems are operated under different ambient conditions.

In order to determine the effect of velocity, independent of air temperature and relative humidity (RH), studies were done resulting in **Figure 6**, which shows the droplet sizes in the center of the plume and the weighted (for water flow) average across the plume. Droplet size measurements were taken at an axial distance of 7.6 cm (3") from the nozzle. The airflow velocity varies from 0 to 15 m/sec (0 to 3000 ft/min).

From **Figure 6**, it can be clearly seen that there is a significant decrease in the measured droplet size when the velocity is increased from 0 and 5 m/sec (984 ft/min). This is due to the fact that the droplet population near the nozzle is very dense and many collisions occur. Collisions result in droplet agglomeration. As the air velocity is increased, droplets of different sizes (with inherently different penetration velocities) are separated into different flow paths and droplet collisions are markedly decreased. At a higher airflow velocity, the smaller sized droplets react quickly to the airflow and take different trajectories as compared to the larger droplets.

To give an idea of the different response times, the largest droplets, of the order of 50 microns, have a response time of less than 8 milliseconds, while droplets of 10 microns have a response time of only about 0.3 ms. Therefore, when the difference between droplet velocity and airflow velocity near the nozzle orifice is around 10 m/s (1,970 ft/min.) a droplet of 50 microns needs 8 cm (3.15") to adjust its velocity to the airflow velocity while a droplet of 10 microns needs only 3 mm (0.12")

At higher air velocities, the center-of-plume measurements become much smaller than the average measurements because more and more of the smaller droplets are pushed towards the center of the plume, due to their faster response time.

Droplet size increases as measurements are taken farther from the orifice (to a limit) because of droplet collisions and coalescence. This increase in droplet size with increasing axial distance (Z) is

shown in **Figure 7**. Note that the effect of higher air velocity, i.e. decreased droplet size due to fewer collisions, is more pronounced close to the exit of the nozzle and diminishes as the axial distance increases until it disappears, for the nozzle tested, at around 20 cm (7.8") downstream from the nozzle exit. Nozzles which produce inherently larger droplets, or which have higher flow rates, can have coalescence effects that continue as much as 50 cm (20") downstream.

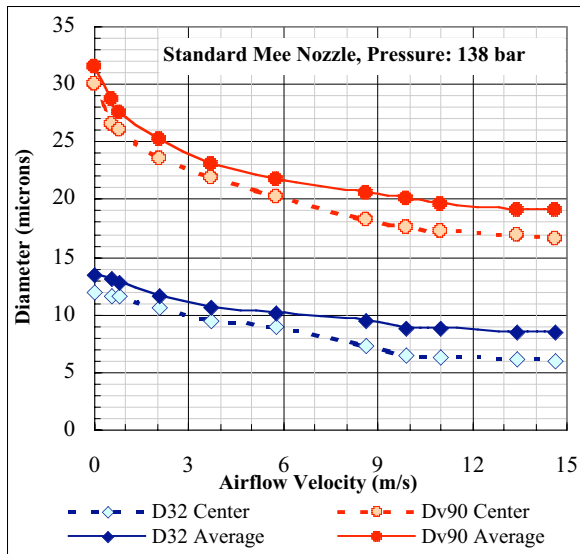


Figure 6. Variation of the droplets size as a function of airflow velocity, measurement were taken at 30°C and 40% RH and at 7.6 cm from the nozzle orifice.

In order to experimentally quantify the effect of rapid small droplet evaporation, measurements were taken at two airflow velocities, 3 m/sec and 13 m/sec (590 ft/min and 2560 ft/min), and for two sets of air conditions; 30°C (86°F) with 40% RH (defined as ambient in the chart) and 20 C (68°F) with 100%RH (defined as saturated).

Figure 7 shows that droplet size near the orifice is not much affected by the psychrometric properties of the air, while the velocity of the air has a dramatic effect. There is only a very small difference in the droplet size measured in cool, saturated air (the solid lines) where evaporation cannot occur, and the size measured in hot, dry air (the solid lines) where evaporation could occur. On the other hand, there is a big difference between droplet sizes at low air velocity (the dark violet lines) and at high air velocity (the green lines.)

Note that the two sets of lines high on the chart show the Dv90 diameters while the two sets of lines lower on the chart give the D32 diameters. The reason for the difference in the two droplet sizes can be understood from the definitions given in **Annex 1**. In studying the curves, one can see that the dashed lines, representing droplet size at non-saturated conditions, start to fall away from the solid lines, representing droplet size with dry air conditions, as the fog moves away from the nozzle orifice. This shows the very small effect of evaporation.

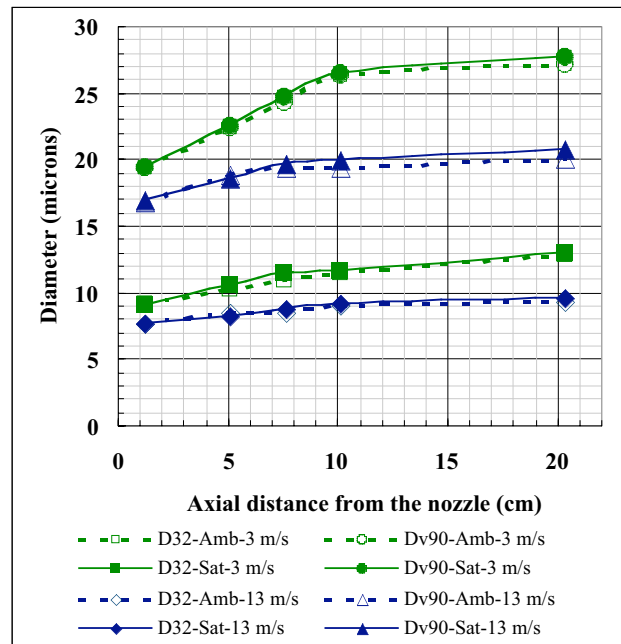


Figure 7. Effect of ambient humidity on droplet size at different axial distances from the nozzle at 138 bar (2000 psi) pressure.

4. EFFECT OF PLUME SHAPE ON DROPLET SIZE

4.1 Pin Dislocation and Droplet size

Concern has been voiced that the dislocation of the impaction pin could cause deterioration in the plume shape that this might result in an increase in the size of droplets produced by the nozzles. First it should be noted that dislocation of the impaction pin nozzle is not easily accomplished due to its structural strength. The pin can be deflected only by striking it a blow with a hard object or by the use of pliers. It is not possible to distort the pins by hand⁴. During installation, the nozzles are protected with plastic caps that are removed only after all work of installation has been finished and the system is ready for operation. The nozzles are unlikely to be damage thereafter, as they are located inside the inlet duct.

In order to understand and quantify the effect of pin dislocation, a nozzle's impaction pin was physically bent using pliers so that the nozzle would produce a distorted spray plume, as shown in **Figure 8**. The photograph clearly shows that the fog in the upper part of the plume is denser than in the lower sector. Detailed measurements of droplet size were then taken in the distorted plume. The nozzle was rotated, in increments of 45 degrees, so as to characterize the droplet size in the plume in all directions.

Droplet tests were done at two airflow velocities and at 1.3 cm (0.5") from the nozzle orifice. Results given in **Figure 9** show that even though the plume looks distorted, the droplet diameter sizes (D32 and Dv90) are remarkably constant. Results for measurements taken at 7.6 cm (3") away from the nozzle orifice, as given in **Figure 10**, also show minimal scatter, about 2 microns. These tests indicate that as long as the impaction pin is above the orifice, even in a non-centered position, the nozzle characteristics do not change

⁴ An axial force of about 200 lbs would result in breakage. Fatigue tests indicate that the pin would have to be distorted back and forth by 120 degrees 8 times before failure.

significantly. Furthermore, nozzles with highly distorted spray plumes are easily found and replaced during system startup or periodic inspections.



Figure 8. Distorted spray plume caused by intentional bending of the impaction pin, 138 bar (2000-psi) operating pressure.

By comparing droplet sizes of the undamaged nozzle shown in figure 7 and the distorted plume nozzle shown in figure 9 and figure 10, one can see that at both distances from the nozzle orifice the measured diameters are essentially the same.

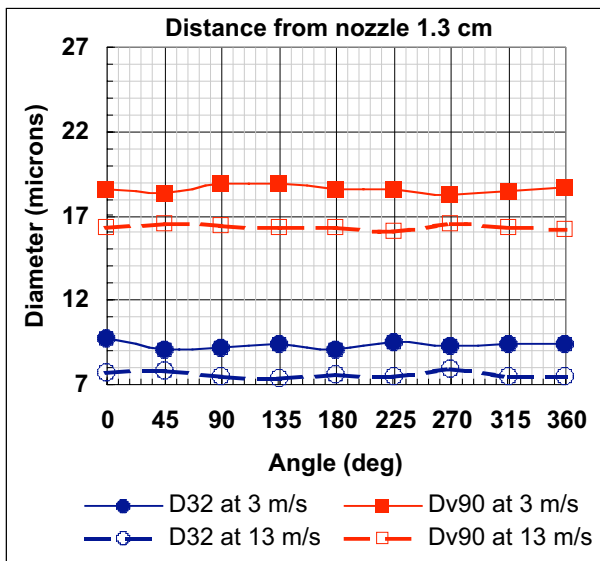


Figure 9 Droplet size at different rotational angles for the distorted-plume nozzle measured at 1.3 cm (0.5”) from the nozzle. Operating pressure is 138 bar (2000 psi).

4.2 Creation of the Nozzle Spray Plume

The shape of the fog plume created by the impaction pin nozzle at different operating pressures was studied in this set of experiments. Close-up, high-speed photographs of the nozzle spray plumes (Figures 12 and 13) were taken in order to better understand plume formation and atomization process. With the impaction-pin nozzle,

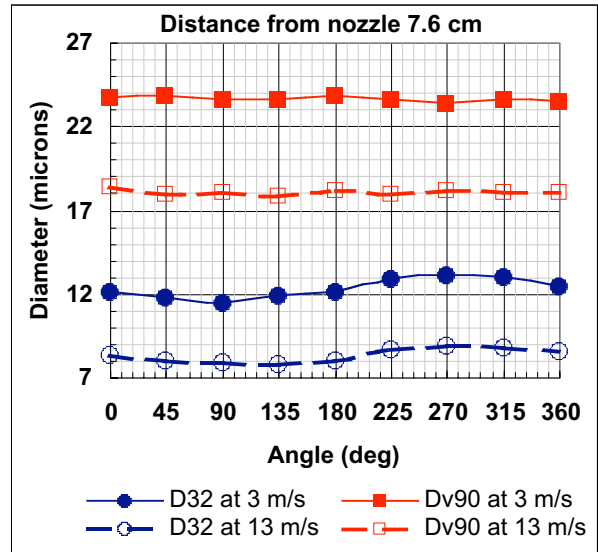


Figure 10. Droplet size at different rotational angles for the distorted-plume nozzle measured at 7.6 cm (3”) from the nozzle. Operating pressure is 138 bar (2000 psi).

water is forced through a short, smooth orifice and hits the impaction-pin at a velocity that depends on the applied pressure. At 138 bar (2000 psi) the water jet exits the orifice at a velocity of about 160 m/s (525 ft/sec). A properly designed impaction pin nozzle splits the water jet when it impinges on the sharp tip of the pin and a thin conically shaped sheet of water is formed. (A poorly designed impaction pin does not form a sheet and produces larger droplets.) The water sheet thins as it expands, then breaks apart into small droplets. Breakup occurs when the aerodynamic forces, which result from turbulence caused by the extremely high velocity of the sheet, overcome the surface tension of the water.

At low operating pressure, surface tension causes the conical sheet to begin to close up. This phenomenon can be seen in Figure 12b where the operating pressure is 34 bar (500 psi). At very low pressures, the sheet closes back on itself and forms a hollow, bulb-shaped structure. As pressure is increased, the momentum of the sheet forces it to open up until it thins to a point where surface tension eventually rips it apart. This results in the formation of fingers or ligaments of water, which then break apart to form small droplets. Finger or ligament formation can be clearly seen in Figure 12a. At pressures higher than about 103 bar (1500 psi), Figure 12f for instance, finger or ligament formation is no longer visible.

4.3 Droplet Formation and the Weber Number

The Weber number is a dimensionless number that is helpful for understanding and predicting sheet or droplet breakup caused by aerodynamic forces. The Weber number is the ratio of aerodynamic forces to surface tension forces and is given by the equation:

$$We = \frac{\rho_a V_{rel}^2 D_d}{\gamma_w}$$

When the Weber number exceeds about 13 [13], the forces of aerodynamic turbulence overcome the force of water tension and breakup occurs. In theory, the mean droplet size produced is estimated to be proportional to the square root of the sheet thickness

at the point of breakup [14]. For a given nozzle increasing the operating pressure increases the sheet velocity so that the point at which sheet break up occurs moves closer to the tip of the pin. This effect is shown in **Figure 11**, which was plotted using measurements taken from the photos in **Figures 12** and **13**.

The conical sheet formed by the impaction pin nozzle expands and slows as it moves through the air. The thickness of the sheet is a function of the orifice and pin geometry and, in the absence of drag would be proportional to the inverse square of the distance from the point of the impaction pin. In the real world, drag acts to increase sheet thickness, or keep it about the same, by causing the sheet flow to backup on itself.

As mentioned above, a thinner sheet will produce smaller droplets, all other things being equal. When operating pressure is increased the point of atomization moves closer to the orifice but the cone angle also increases. At this new point of atomization the sheet is probably actually thinner so that smaller droplets are produced. This agrees with our empirical data, which shows smaller droplets and higher flow rates for increasing operating pressure.

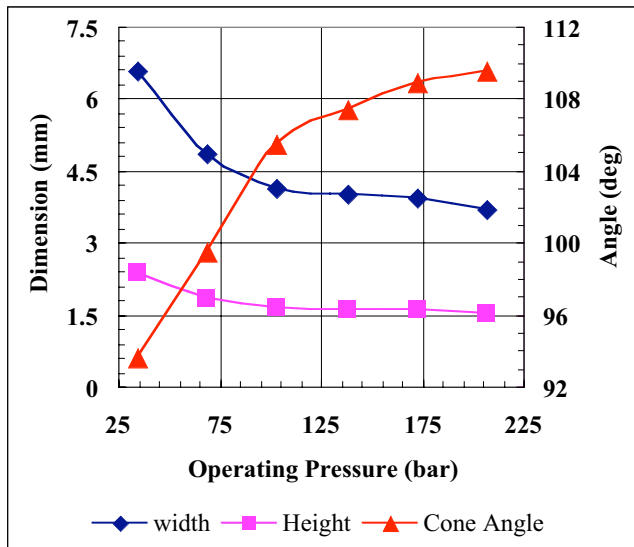


Figure 11, Cone angle, height and width of the conical water sheet at the point of atomization.

The Weber number seems to approximately apply to the sheet break up for the nozzle being discussed. If we assume demineralized water at normal ambient temperature and standard atmospheric air, then the term ρ_a/γ_w is equal to about 17.36. If we assume the sheet velocity is about 100 m/s (328 ft/sec) at the point of atomization (i.e. we assume that it has slowed considerably from its initial velocity of 160 m/s) and assume a sheet thickness as 75 microns [75×10^{-6} m] (i.e. assume it has not thinned) then we get a Weber number of 13. In fact any combination of sheet velocity and thickness, the product of which is equal to 0.75, will yield a Weber number of about 13. But since we know the velocity didn't increase and we know the sheet thickness is of the order of 75 microns, we can approximately determine the Weber number.

The Sauter Mean Diameter (SMD or D32) of a fog spray is reported to be approximately equal to the square root of the thickness of the sheet at break up. Using the laser particle analyzer described above, the SMD for this nozzle was found to be about 9 microns. In

the above approximation we assumed a sheet thickness of 75 microns, at 138 bar (2000 psi). The square root of 75 is 8.6, which shows a surprising degree of agreement with the measured values. Confirming these approximations will be the subject of future research at Mee Industries.

5. NOZZLE SPRINKLE AND PIN SHADING EFFECTS

When operating pressure is low, the impaction-pin nozzle may exhibit large droplet formation, which we call sprinkle. A detailed study of large droplet formation was conducted and results are given here. Sprinkle occurs when the conical water sheet contacts the wider portion of the impaction pin. Airflow or gravity eventually strips these very large droplets off the pin and they are broken up by collision with the high velocity spray plume.

Sprinkle formation can be seen in the photos in **Figure 12**, which shows spray plumes generated at operating pressures ranging from 34 to 103 bar (500 to 1500 psi). One can see that the size of drops emitted from the pin decreases significantly and becomes almost invisible at the higher pressures. Looking at **Figure 13** we see that, at 138 bar (2000 psi), sprinkle formation has completely disappeared.

The quantity of water emitted from the pin as larger droplets (sprinkle) was estimated at an operating pressure of 34 bar (500 psi) by estimating the size of the droplets and counting the rate of formation. It was observed that droplets of about 2 mm were produced at the rate of about one per second, which equates to about 0.3% of the total mass flow of the nozzle. The 2 mm droplets shatter when they are ejected into the vigorous spray plume and smaller droplets are formed. The laser particle analyzer is capable of measuring droplets up to 400 microns, with its current lens configuration, but since the mass flow is so low the large-droplet data has only a negligible effect on the measured droplet size.

During nozzle testing in the wind tunnel it was noticed that swirl jet nozzles also produce sprinkle. The lower exit velocity of the swirl jet nozzles results in some very small droplets being re-circulated back to the face of the nozzle where they agglomerate and eventually form a large droplet. When this droplet reaches a critical size it falls off the nozzle or is suctioned back into the spray plume where it is shattered into smaller droplets. This mode of sprinkle occurs even at the higher operating pressures. No attempt was made to quantify the amount of sprinkle from a swirl jet nozzle but it is probably also a statistically insignificant amount. It was also noted that impaction pin nozzles other than the Mee nozzle, which do not have good sheet formation, produce sprinkle even at high operating pressures.

In the typical operating range for impaction pin nozzles, which is 140 to 210 bar (2000 to 3000 psi), the sprinkle effect either goes away completely or is too small to be visible. This is because at higher operating pressures the point of atomization occurs before the water sheet reaches the pin and the fog droplets are small enough to follow the flow lines around the pin.

Our conclusion is that sprinkle from impaction pin nozzles is either non-existent or insignificant at normal operating pressures.

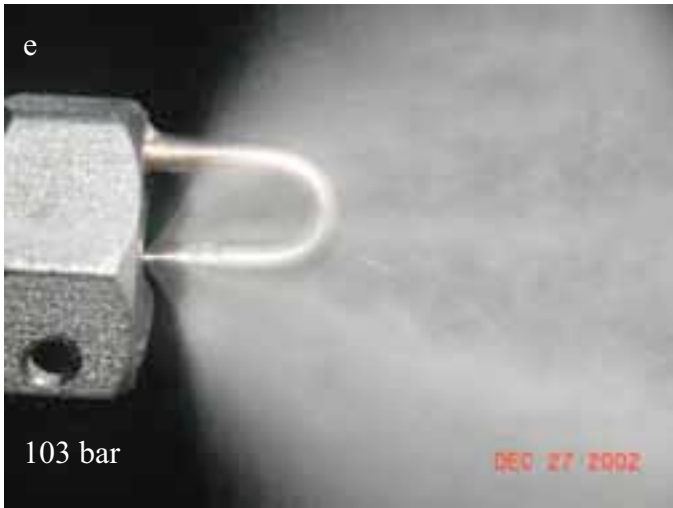
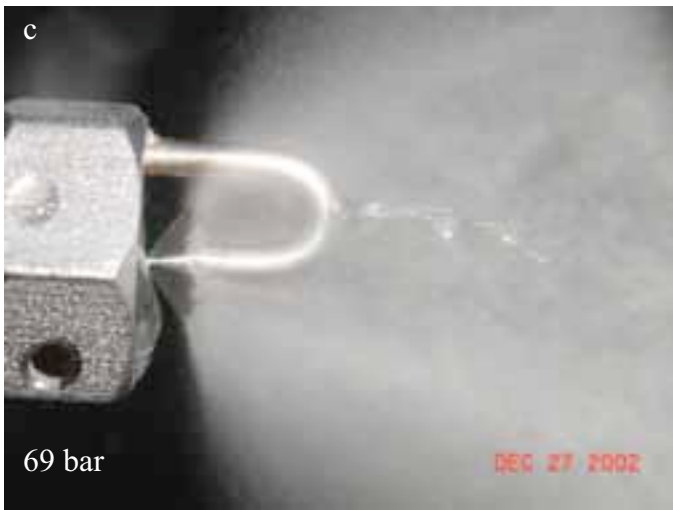
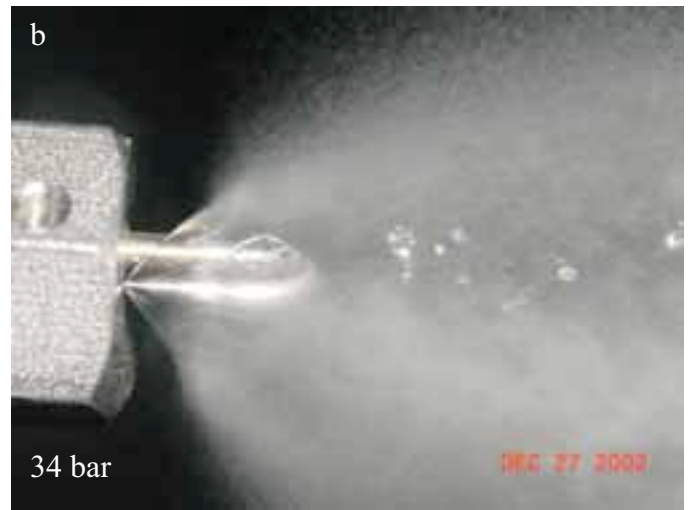
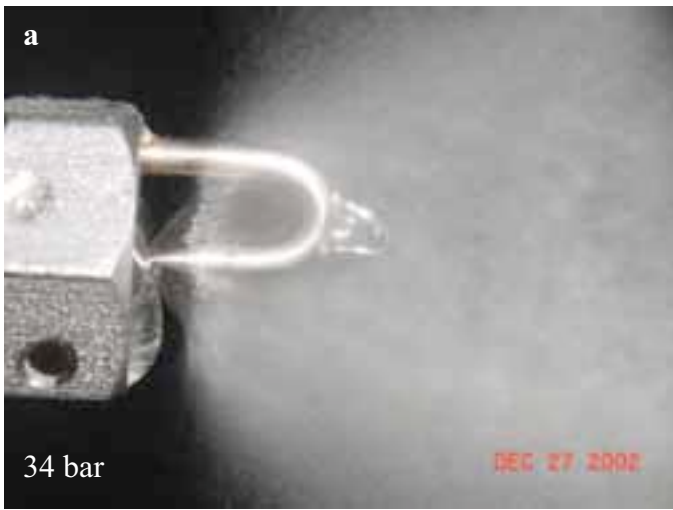


Figure 12. Sprinkle effect from a standard Mee nozzle at operating pressures from 34 bar to 103 bar (500 to 1500 psi). The views on the left are facing the impaction pin and on the right in line with the impaction pin. Note how sprinkle lessens with increasing operating pressure.

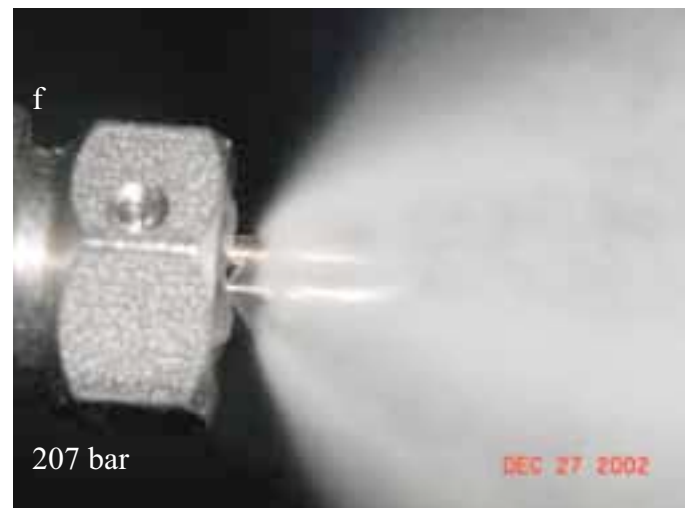
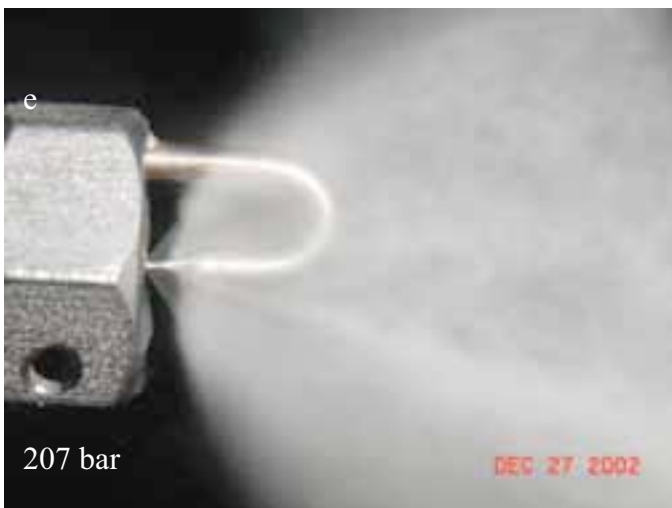
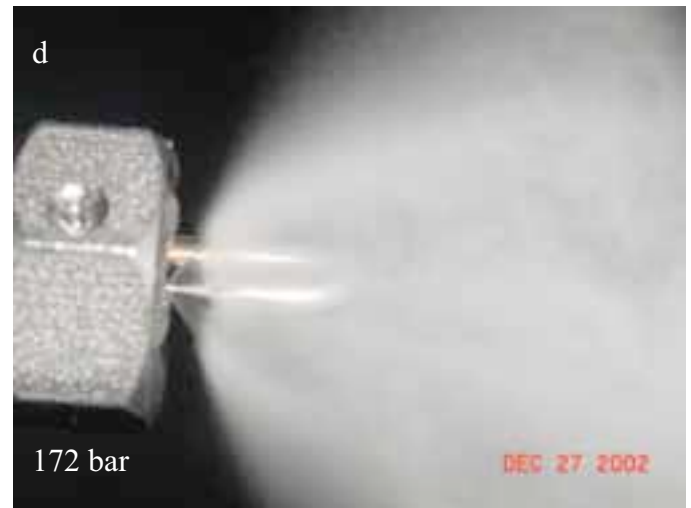
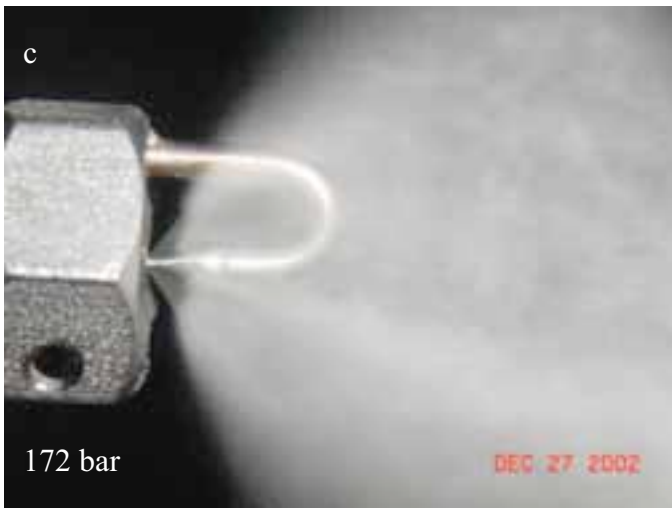
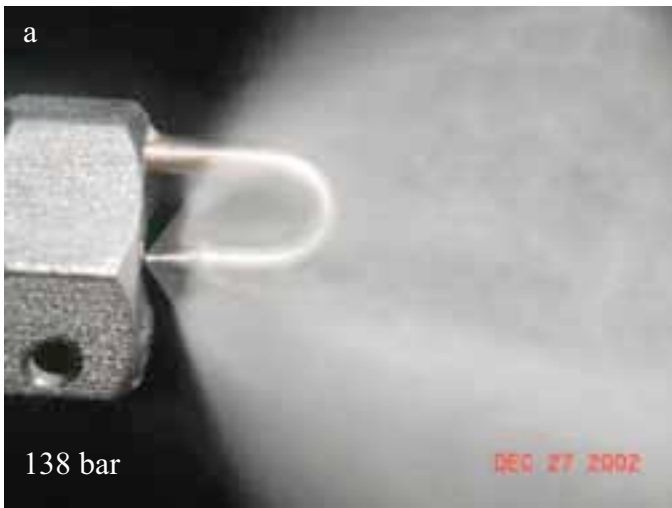


Figure 13. Standard Mee nozzle spray plumes at operating pressures from 138 to 207, bar (2000 to 3000 psi). Note the absence of larger droplets (sprinkle) at these operating pressures. One can also clearly see that the atomization process begins well before the spray plume contacts the support side of the impaction pin.

6. DROPLET HEAT AND MASS TRANSFER MODEL

Before trying to understand the complex properties and behavior of the whole mass of fog droplets emitted from the nozzle, it is helpful to study the properties and behavior of individual droplets. This understanding can then be extended to study the interaction between a single droplet and the other droplets and their interaction with the carrying phase (air). The study of an isolated droplet is first treated using the classical assumption of spherical symmetry for both the liquid droplet and the surrounding air. The behavior of a single droplet injected into the airflow will first be analyzed, then a study of the effect of the velocity on droplet thermodynamics and trajectory will be done.

A numerical model of droplet behavior was developed (Chaker et al [1]). This model works in iterative manner and provides the transient behavior of fog droplets in terms of the droplet diameter, change in relative humidity and temperature and time to attain saturation. The iterations stop ($i=i_{max}$) when the air in the volume around the droplet within Active Radius (RA) becomes saturated or when the droplet evaporates completely. The process is shown in the flow chart of **Figure 14**.

The model makes a quantitative analysis of fog droplet behavior in gas turbine inlet ducts possible. As soon as a droplet touches the air, and if the vapor pressure near the droplet surface is higher than the vapor pressure of the air far from the droplet (i.e. the droplet is in unsaturated air), evaporation of the droplet starts to occur. In order to balance the evaporation (mass transfer), the droplet has to lose a quantity of energy (heat transfer), which reduces the temperature of the droplet and of the air surrounding it. Depending on the droplet relative velocity, either natural or forced convection will occur. Natural convection occurs when the relative velocity of a droplet compared to the surrounding air is zero, and forced convection occurs when a relative velocity differential exists.

The effect of velocity on evaporation is not significant in our conditions (the effect is less than 10% for 50 microns droplet and further decreases when the droplet size diminishes) because the droplets are very small and their response time, in our experimental conditions, is lower than 10 ms [3]. This means that the use of single droplet model gives a good estimation of the behavior of all the droplets in the duct.

6.1 Model Results and Discussion

The basic model was described in detail in Chaker et al [1] and it has now been extended so it may be applied to the entire distribution of droplets. The droplet size distributions collected by the laser particle analyzer typically have 30 to 40 classes of droplet size. By calculating the evaporation time of each size class, it is possible to calculate the evaporation efficiency of the entire distribution. The basic procedure is as follows: First we insert into the model the volume percentage of all the size classes and other initial data such as droplet temperature and the psychrometric parameters of the air. Second, we calculate the evaporation rate of each size class and then, by multiplying each class by the percentage of the volume of water evaporated, we calculate the new initial conditions and iteratively reinsert them in the model, until the final solution is derived.

The results are shown in **Figures 15, 16 and 17**, which are discussed in detail below. Taking into account the different ambient

psychrometric conditions that may typically exist with inlet air-cooling in different climate zones, based on analysis done by Chaker et al [15, 16], three initial ambient conditions have been considered:

45 C (113°F) and 5% RH: Hot and dry (HD) desert weather conditions with evaporative cooling potential of 26°C (47°F)

30 C (86°F) and 55% RH: Typical temperate climate summer condition with cooling potential of 8 °C (14.4°F)

15 C (59°F) and 80% RH: Cold and Humid (CH) weather conditions with 2°C (3.6°F) of cooling potential.

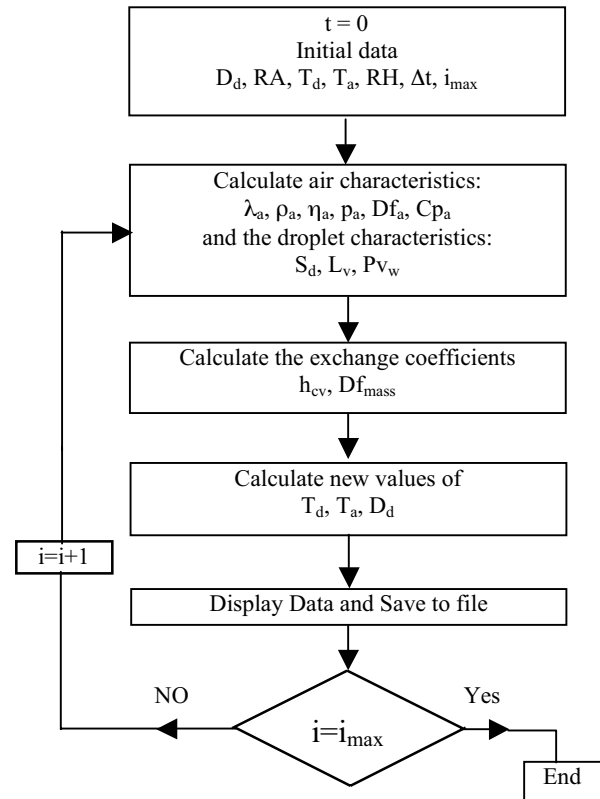


Figure 14. Computational Model for Droplet Evaporation

6.1.1 Discussion of Evaporation Dynamics for Single Droplets

A set of curves that show the behavior of individual fog droplets at the three different initial ambient conditions are given in **Figure 15** (note that $T_{a,i}$ and $RH_{i,i}$ refer to the initial air temperature and relative humidity, respectively). In the charts on the left side of the figure (a, c and e), the abscissa is the initial droplet diameter ($D_{d,i}$) and the ordinate provides the time required to reach the humidity level given by the different curves.

In the charts shown on the right side (b, d and f), the abscissa is again the initial droplet size and the ordinate is the droplet diameter at the point time when the humidity given in the different curves is reached. The curves give an understanding of fog droplet evaporation as noted in the observations ahead:

In examining **Figure 15a**, let us consider an initial droplet size of 20 microns. We enter the abscissa at 20, move upwards to an RH of 95% and find, on the ordinate, that reaching this RH took about 1.1 seconds. Moving to **Figure 15b**, and entering the abscissa, again at 20 microns, we move up to the 95% RH curve and, reading from the ordinate, we note that the droplet evaporated down to a diameter of about 4 microns.

Doing the same exercise with **Figure 15c** we see that with cooler and moister ambient conditions the time required to attain 95% RH with a 20-micron droplet increases to about 2 seconds. And moving to **15d** we see that evaporation to 95% RH reduced the 20-micron droplet to just 9 microns.

In examining charts we see the critical importance of droplet diameter. For example if we start with droplets of 40 microns, and assume that we have only one second residence time before the droplet reaches the compressor (typical for an inlet fogging system), we see that the relative humidity has been increased only to 60% and the remaining droplet is still more than 30 microns in diameter. Obviously an inlet fogging system that produced droplets in the 40-micron range would not be very efficient and would introduce large droplets to the compressor.

We can see that ambient conditions play a major role in speed of evaporation. With typical summer time conditions for a temperate climate (**Figures 15c and d**), the time required to reach 95% relative humidity increases to 2 seconds and the remaining droplet is 9 microns. Contrast these values with the values for the desert climate, given in the example above, where they were 1.1 seconds and 4 microns.

6.1.2. Discussion of Evaporation Efficiency for Entire Spray

The Volume frequency and cumulative volume for two initial ambient cases of 45 C (113°F) with 5%RH and 15 C (59°F) with 80% RH are shown in **Figure 16 and 17** respectively. These charts are based on a 1 second residence time, as that is typical for gas turbine inlet ducts. The charts were constructed using the curves of **Figure 15** and computing the evaporative efficiency for each different class of droplet sizes. This allows a determination of the evaporated water and non-evaporated water that would be expected from fog systems. Between 30 and 40 classes of droplet diameter were considered, depending on the range of droplet size distribution.

The most important quantitative factors for the fog spray are the surface area of water exposed for evaporation (which affects the evaporative cooling efficiency of the spray) and the size of the largest droplets (which affects the potential for compressor blade distress as well as giving in indication of the amount of water that will fall out in the duct) [2,3]. Given the above, the SMD, which is equal to the volume-to-surface-area ratio of the entire spray, and the Dv90 numbers are of primary importance. However, The presence of a large number of small droplets, which can represent a negligibly small quantity of injected water, can significantly reduce the D32 value. Since the total mass of small droplets is insignificant for the cooling process, using SMD alone can be misleading. When comparing two different nozzles it's best to use Dv90.

DV90 is relatively unaffected by numerically large populations of small droplets, that may represent a very small collective mass. Therefore, Dv90 was used to select typical droplet size distributions to characterize the evaporation efficiency of injected water droplets.

In **Figures 16 and 17**, data has been provided for three different fog droplet distributions with Dv90 diameters of about 18, 28 and 46 microns. These distributions were chosen as being representative of nozzles that have been applied for inlet fogging (the 18-micron distribution being representative of that produced by Mee nozzles at 138 bar, or 2000 psi).

In **Figure 16a and b**, the initial Dv90 diameter is 18.5 microns, it can be seen that the total injected water (the blue line) and the evaporated water (the red line) follow the same curve, and therefore the non evaporated water (the green line) is at zero. In **Figure 16c and d** with a Dv90 of 28.1 microns, we see that there is some separation of the blue and red lines. In **Figure 16d**, we see that the evaporated water curve never reaches more than 95%, so the un-evaporated water is about 5%. The remaining spray has a Dv90 size of up to 39 microns. The reason for the increase in Dv90 (from 28 to 39 microns in this case) is the fact that the smaller droplets evaporate to zero, while the largest droplets get only slightly smaller. **Figure 16 e and f** shows a Dv90 of 46.2 microns, the un-evaporated water increases to 14% and the Dv90 size of the non-evaporated droplets is as high as 59 microns.

Figure 17 is similar to **Figure 16** except that the initial psychrometric conditions are much cooled and moister. The picture changes significantly. In examining **Figure 17a**, we see that the majority of the un-evaporated water (the green line) consists of droplet sizes between 10 and 30 microns and the maximum volume percentage of un-evaporated droplets are in the 17-micron size class. In looking at **Figure 17b**, one can see that 25% of the water did not evaporate. This is very interesting when viewed in comparison with the hot and dry climate conditions (**Figure 16a and b**) where all the fog evaporated. Looking at the graphs of **17c and e**, where the initial droplet size is 46 microns, we see that the amount of non-evaporated water increases significantly (to almost 70%), as does the maximum final droplet size (80 microns).

It is important to note here that the size of un-evaporated droplets for a Dv90 distribution of 18.1 microns varies between 10 and 30 microns, while this number increases to between 10 and 50 microns for a Dv90 distribution of 28.1 microns and reaches a value between 10 and 80 microns for a Dv90 distribution of 46.2 microns. In addition to the decrease in evaporation efficiency the considerably higher Dv90 may also have a negative impact on compressor blade life.

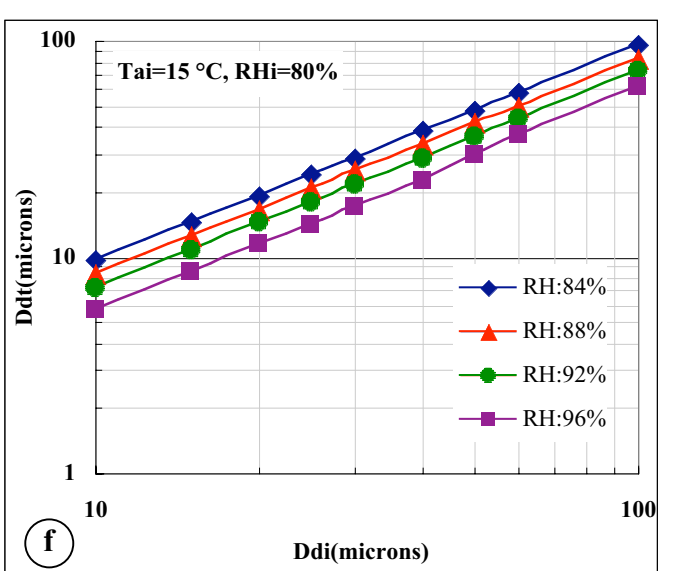
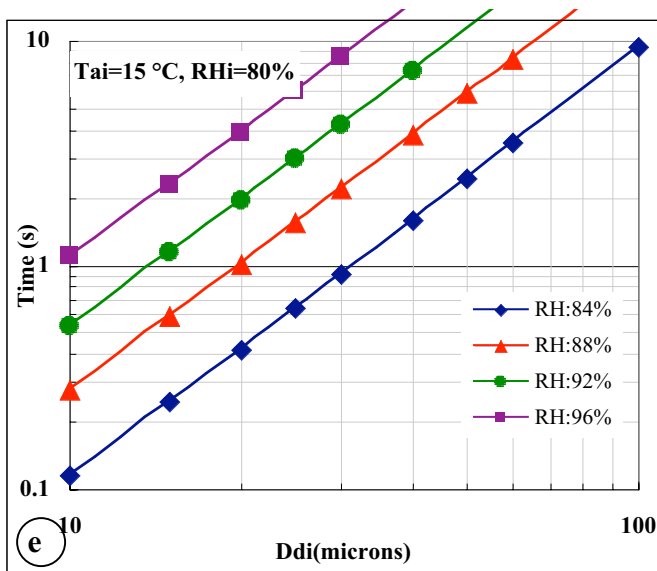
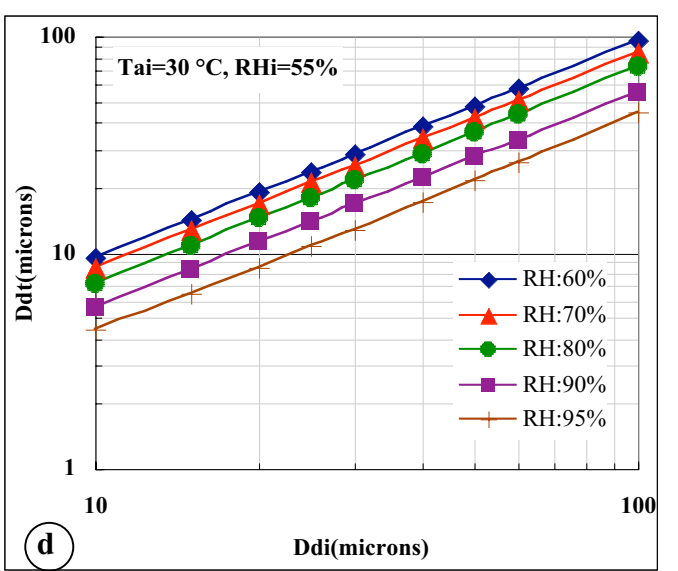
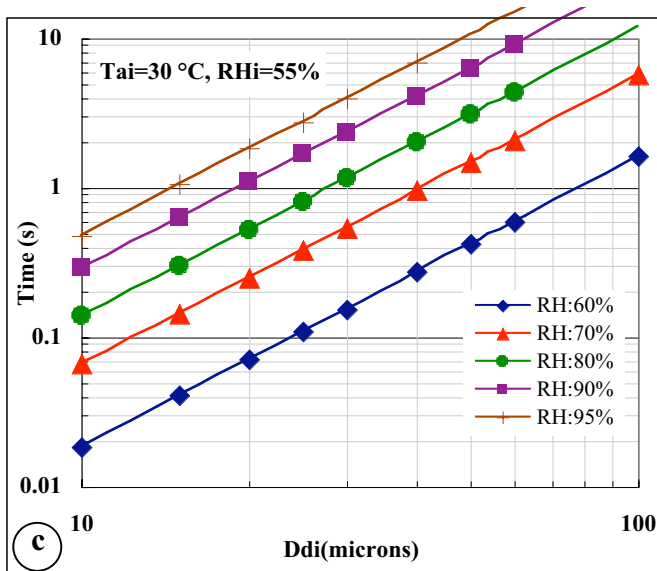
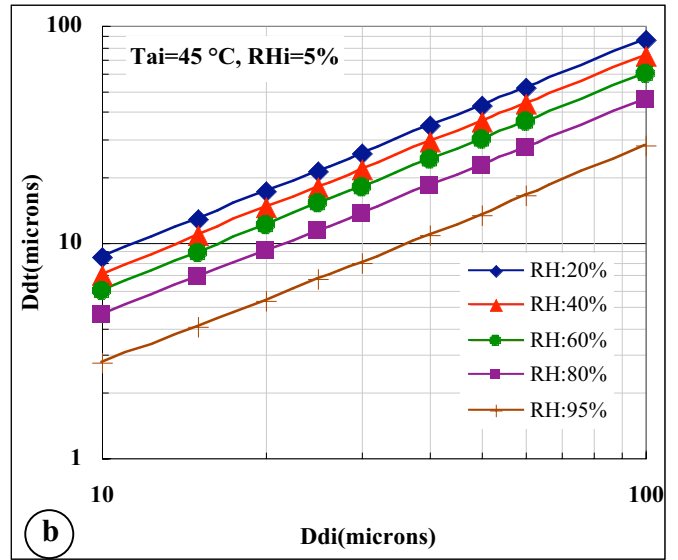
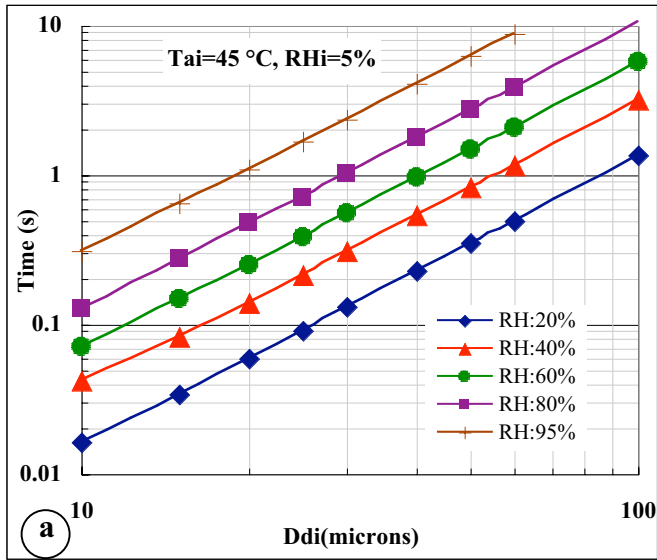


Figure 15. Evaporation curves for single droplets showing residence time requirements, ending RH, and final droplet sizes for 3 ambient conditions.

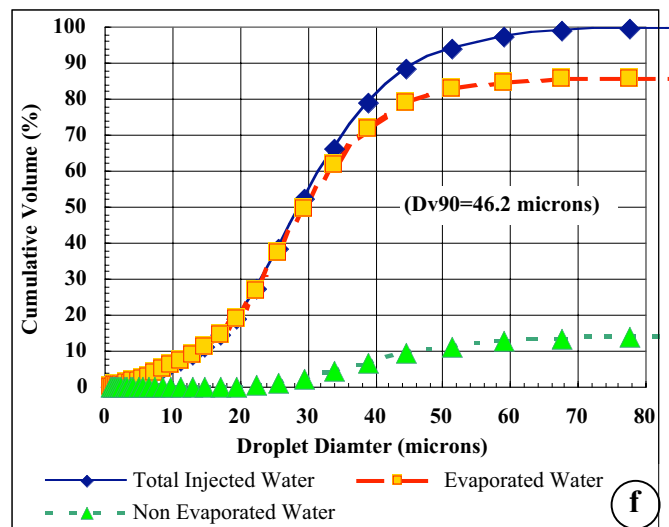
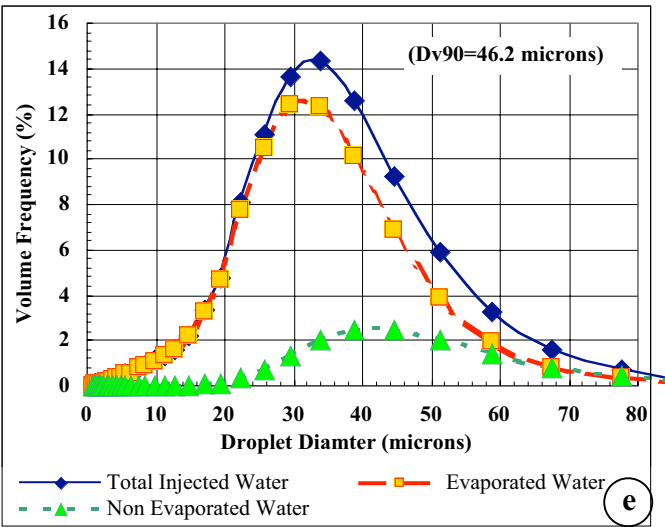
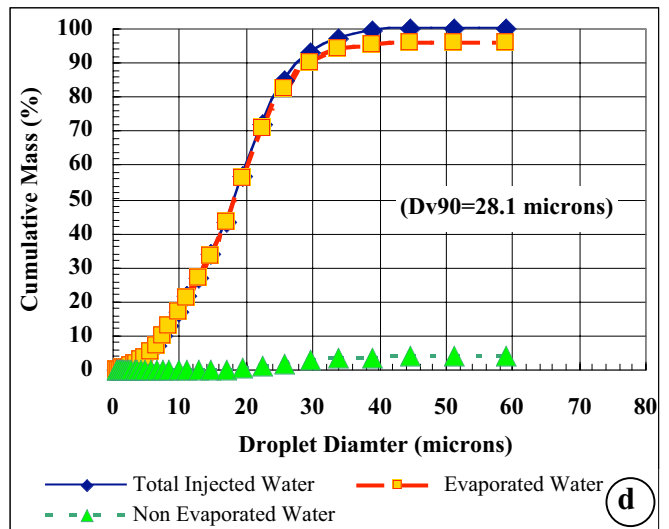
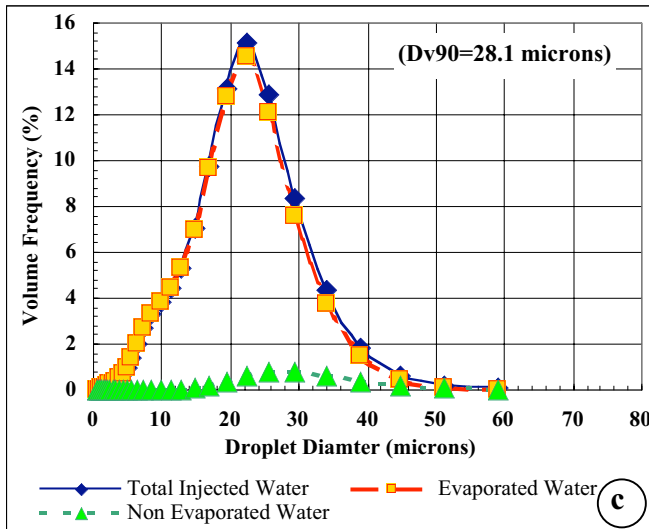
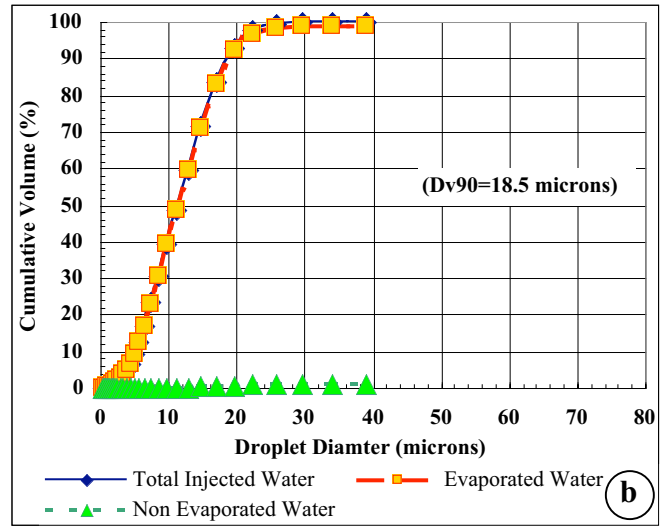
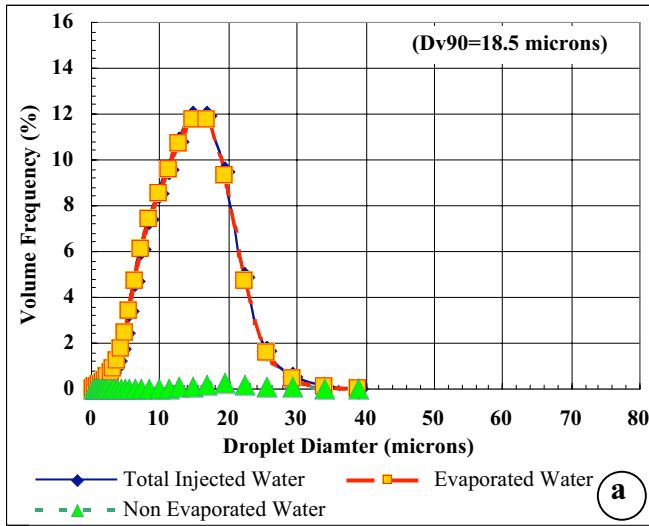


Figure 16. Volume distributions showing total injected water, un-evaporated water and evaporated water for ambient conditions of 45 C (113°F) with 5%RH and one second residence time. The curves on the left (a, c and e) show the volume frequency and curves on the right (b, d and f) provide cumulative volume.

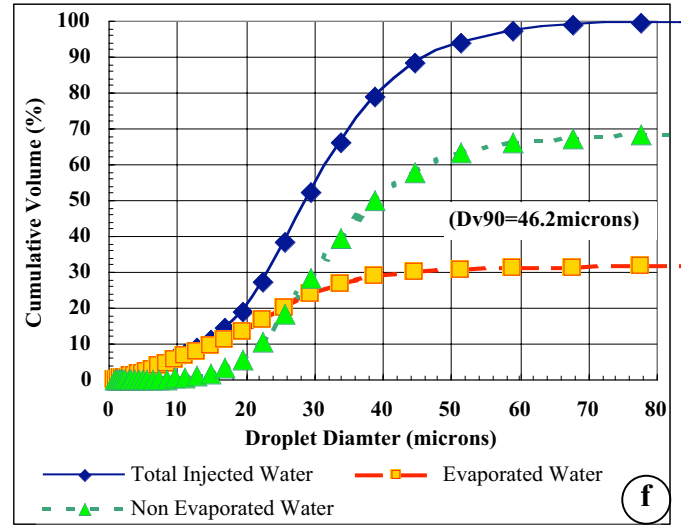
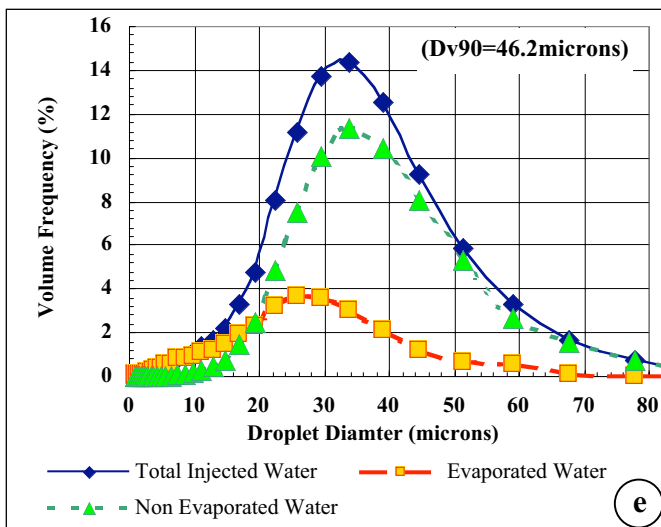
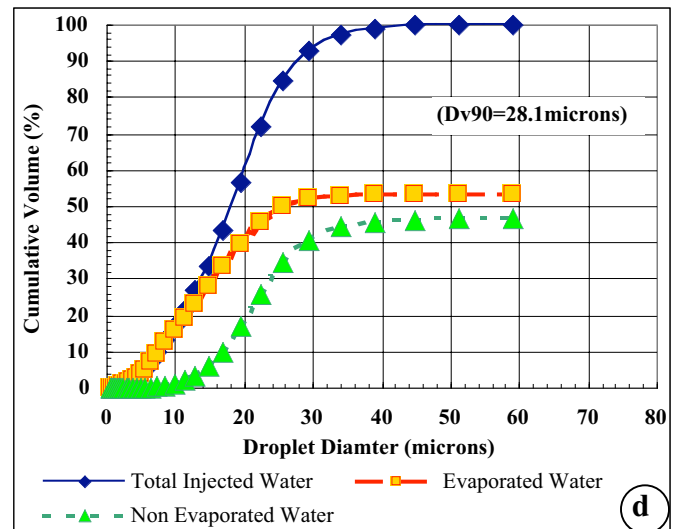
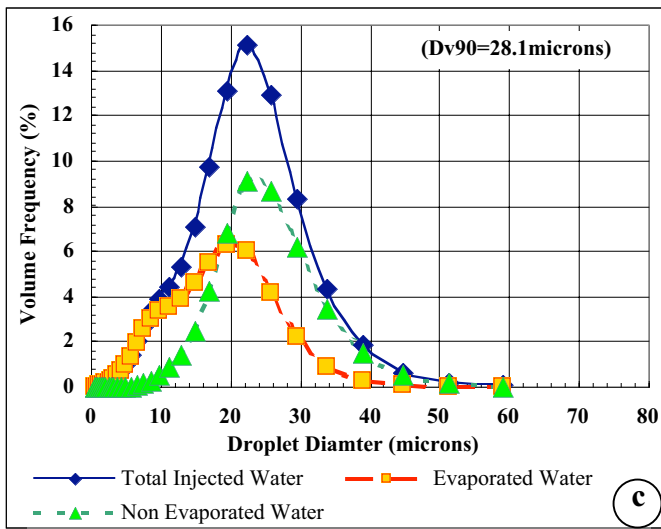
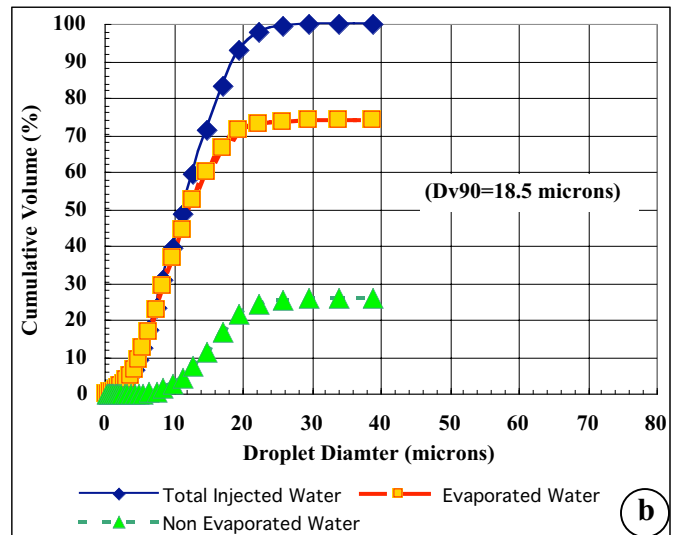
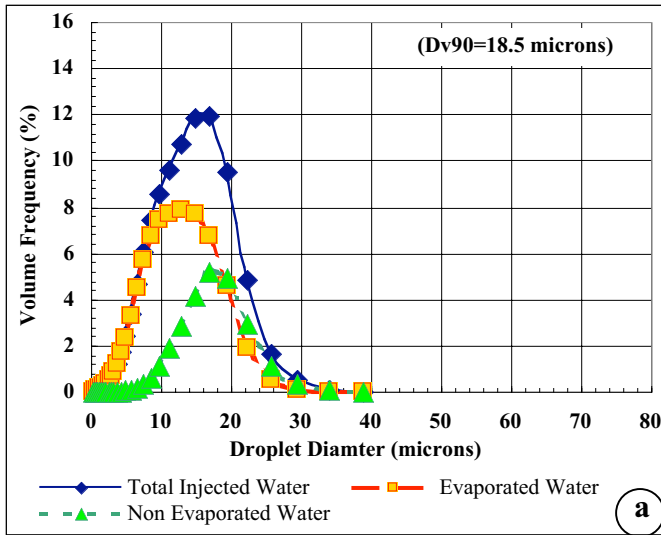


Figure 17. Volume distributions showing injected water, un-evaporated water and evaporated water for ambient conditions of 15 C (59°F) with 80%RH and one second residence time. The curves on the left (a, c and e) show the volume frequency and curves on the right (b, d and f) provide cumulative volume.

7. CONSIDERATIONS RELATING TO POSITIONING OF NOZZLE MANIFOLDS.

The position of the nozzles manifold in the duct should be chosen with care. In general there are three positions in the gas turbine duct where nozzle manifolds could be installed.

Close to the inlet filter housing where the airflow velocity is around 2.5 m/s (500 fpm), this position is commonly used for evaporative fogging applications.

After the silencer where the velocity is around 12.7 m/s (2500 fpm). This position is used for evaporative fogging and for combined overspray fogging.

In the duct close to the axial compressor inlet, which is the typical overspray installation, where the residence time will be of the order of 0.2 seconds. The velocity here would also be close to 12.7 m/s (2500 fpm)

Installing the fog manifold close to the inlet filter housing, the airflow velocity is low, leads to longer residence time and, therefore, better evaporative cooling efficiency. However, the fog spray is poly-dispersed so the penetration velocity of the bigger droplets emitted from the nozzle orifice is higher than the penetration velocity of the smaller ones and, consequently, droplet collision and coalescence occurs.

By installing the nozzle manifold after the silencer, the coalescence effect is reduced significantly due to the fast response time of the smallest droplets to the high airflow velocity. Large and small droplets are separated into different flow paths and collisions are greatly reduced. The higher Weber number may also lead to secondary droplet breakup. A typical nozzle that produces a Dv90 of 25 microns at the lower velocity of the air-filter house will produce a Dv90 of 20 microns in the higher air velocity that exists after the silencer. By installing the nozzles manifold after the silencer however, the residence time of the droplets in the duct is typically reduced from 1 second to just 0.3 seconds.

Given the above, the position of the nozzle manifold in the duct should be chosen by taking into account the trade-off of droplet size and residence time in the duct. Since all the droplets are small enough to quickly take the velocity of the airflow, the effect of the velocity itself on the evaporation rate is negligible. In cases where maximum evaporation efficiency, minimum fallout and no overspray are desired, locating the nozzles in the filter house will almost always be the better option.

An example is provided here for a hypothetical gas turbine with a mass flow rate of 500 Kg/s, with ambient psychrometric conditions of 30°C (86°F) and 20% RH and with a fog injection rate of 5 kg/s. Only 3 kg/s of water are required to saturate the 500 kg/s airflow so the remaining 2 kg/s of water (0.4 % of total airflow) becomes overspray.

By using the droplet size distributions measured at 2.5 m/s (filter-house velocity) and 12.7 m/s (duct velocity), calculations were made to determine the quantity of water that will be evaporated within 1.2 seconds (for the 2.5 m/s distribution) and 0.2 second (for the 12.7 m/s distribution).

The results for a residence time of 1.2 seconds are shown in **Figures 18 and 19**. In looking at **Figure 18**, the un-evaporated water has droplet distribution sizes of 18-40 microns. The un-evaporated water (overspray) will reach about 5% of the total injected fog, as can

be seen in **Figure 19**. The evaporation efficiency (using the active radius approach) after 1.2 seconds, with ambient conditions of 30°C (86°F) and 20% RH and using the size distribution measured at 2.5 m/s, is 94.4% (Red curve in **Figure 19**). The Dv90 as can be seen from **Figure 19** is 25 microns.

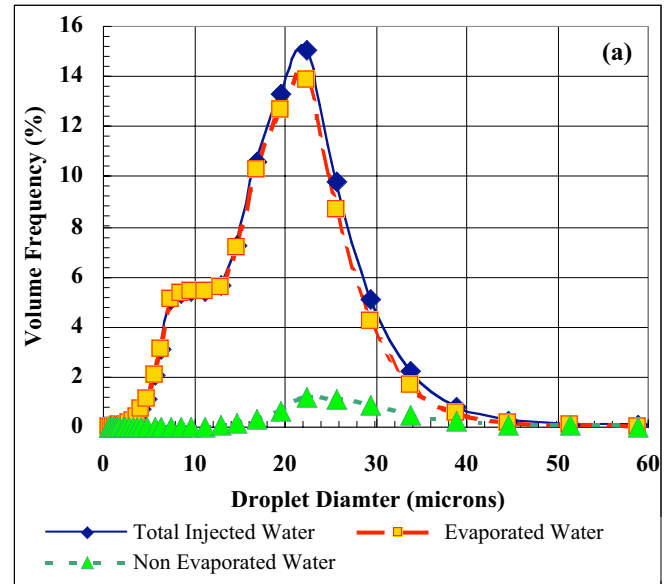


Figure 18. Volume frequency of droplets from nozzles located in a low velocity region (filter house), residence time is 1.2 seconds

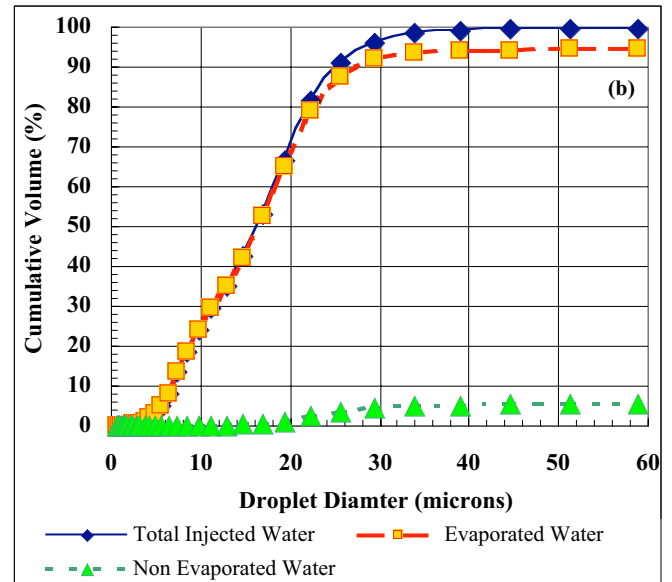


Figure 19. Cumulative Volume frequency of droplets from nozzles located in the low velocity region (filter house), residence time is 1.2 seconds. Evaporation efficiency is 94.4 %.

The corresponding figures for a shorter residence time of 0.2 seconds are shown in **Figures 20 and 21**. The evaporation efficiency after 0.2 second, using the size distribution measured at 12.7 m/s, drops to 77.3% as show in **Figure 21**. The amount of un-evaporated water is approximately 22% and the Dv90 is 20 microns.

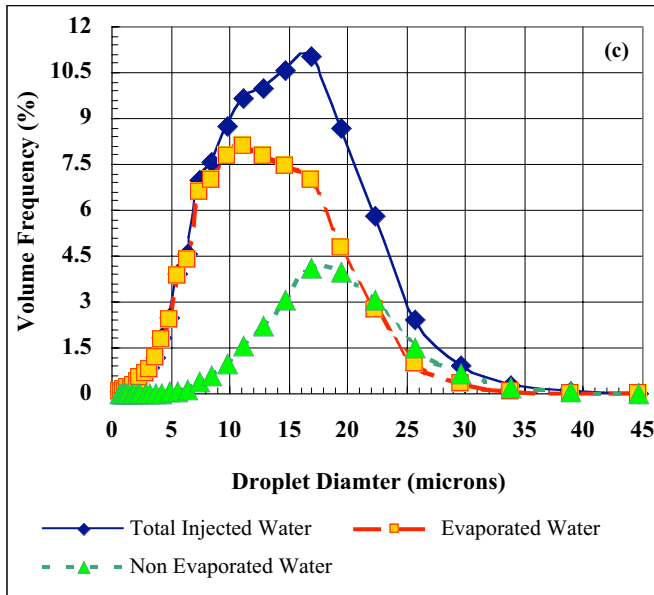


Figure 20. Volume frequency of droplets for nozzle located in the high velocity region of the duct (after silencers), residence time of 0.2 seconds

In this conditions, the installation of the nozzles manifold in the inlet filter housing leads to a better evaporation efficiency (94.4%) compared to the second position close to the axial compressor inlet with an evaporation efficiency of 77%.

By injecting 5 kg/s (0.4 % Over spray), it is clear that we can reach saturation in both cases ($0.94 \cdot 5 = 4.7$ Kg/s in the first case, and $0.77 \cdot 5 = 3.9$ kg/s in the second case) and only 3kg/s is required to reach saturation. Therefore the wet bulb temperature is reached in both cases.

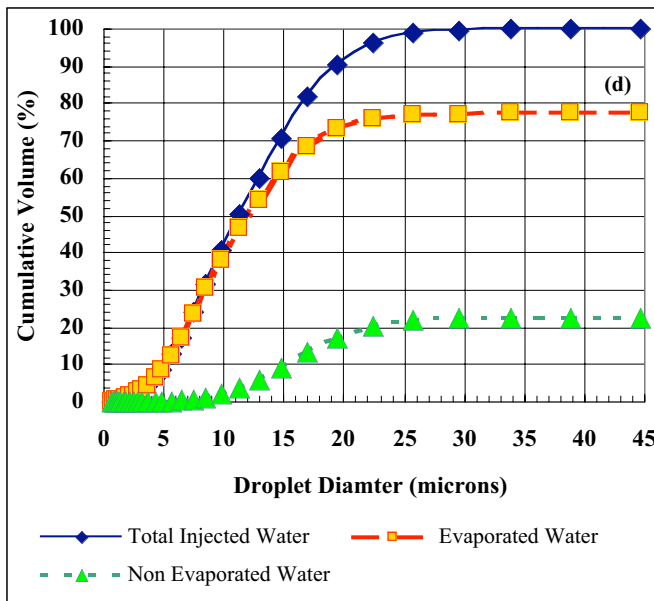


Figure 21. Cumulative Volume frequency of droplets from nozzles located in the high velocity region (after the silencers). Residence time is 0.2 seconds. Evaporation efficiency is 77 %

7.1 Generalized Curve for Evaporative Efficiency

In order to generalize the results showing evaporative efficiency and residence time, **Figure 22** has been constructed. Two sets of climate conditions have been considered defined as:

- Hot and Dry (HD) – top three solid curves
- Cold and Humid (CH)- lower three dotted curves.

Considering a residence time of 1 second and assuming a hot and dry day, the evaporative efficiencies will range between 85- \approx 100% for sprays with a Dv90 ranging from 18-46 microns. Even on a cold and humid day, this would hold true for Dv90 of 18.5 microns, while the evaporation efficiency decreases to around 32% for a Dv90 of 46.2 microns.

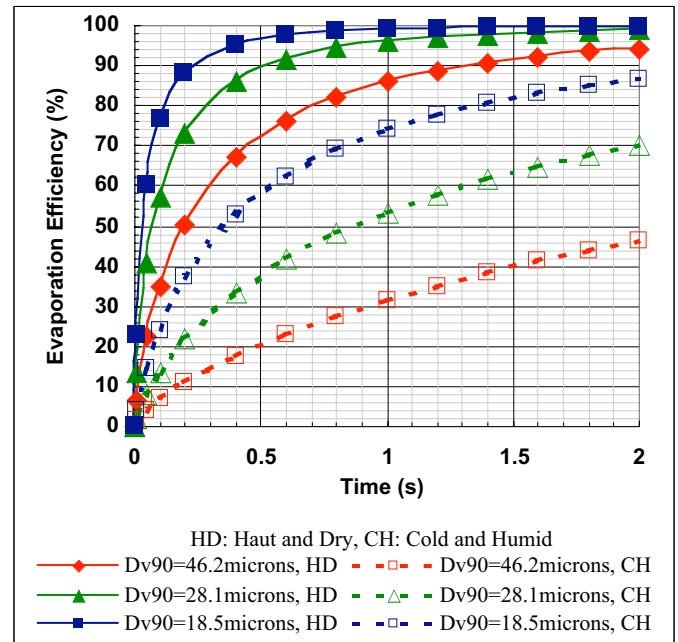


Figure 22. Summary curve showing evaporative efficiency for a range of residence times and Dv90 droplet sizes

7.2 Experimental Verification of the Evaporative Efficiency Model.

Experimental testing was conducted in the wind tunnel to validate the results of the theoretical evaporation efficiency model. The results of this are shown in **Figure 23**. In this figure, the solid blue line is the evaporation efficiency predicted by the model and the experimental test points are also provided. It can be seen that there is a close correlation between the results predicted by the evaporation model [1] and the experimental results from experiments conducted in the wind tunnel at different airflow velocity and ambient conditions.

In examining the fit between the predictive model and the actual test results, it can be seen that the model slightly under-predicts evaporative efficiency at the lower residence time (for example the data point around 0.4 sec residence time). The model slightly under predicts efficiency for residence times ranging from 0.9-1.5 seconds.

The reason for this is that the model assumes that each drop has the required volume to saturate the air around it but in reality, this is not the case. Close to the nozzle the droplet population is very dense and also there will be some regions of untreated air between the nozzles. Therefore the model tends to overestimate the evaporative efficiency for very short residence times. As the residence times increase, the small droplets tend to evaporate faster thus increasing the relative humidity so making evaporation of the larger droplets more difficult. It is important to note that the deviations are exceedingly small, however a physical explanation has been provided to understand the reasons for the deviation. Work is underway to extend the model further to incorporate these factors.

This model was verified using experimental data from a wind tunnel. The experiments were done without the presence of a silencer or any other obstructions such as trash screen or heating tubes. In real gas turbine ducts, the impact of large droplets with these obstructions, may lead to a decrease in evaporation efficiency and an increase of the Dv_{90} of the non-evaporated fog droplets. Due to the large variations of geometry of gas turbine inlet configurations it is not practical to simulate them all. Each configuration needs to be treated on a case-by-case basis. The model extension planned will incorporate these effects.

Depending on the inlet duct geometry, the airflow velocity may vary between the different regions in the inlet duct [17], and the fog nozzle should, therefore, be distributed in such a way to take into account this difference in airflow velocity. Such distributions will aid mixing and reduce temperature deformation at the compressor inlet.

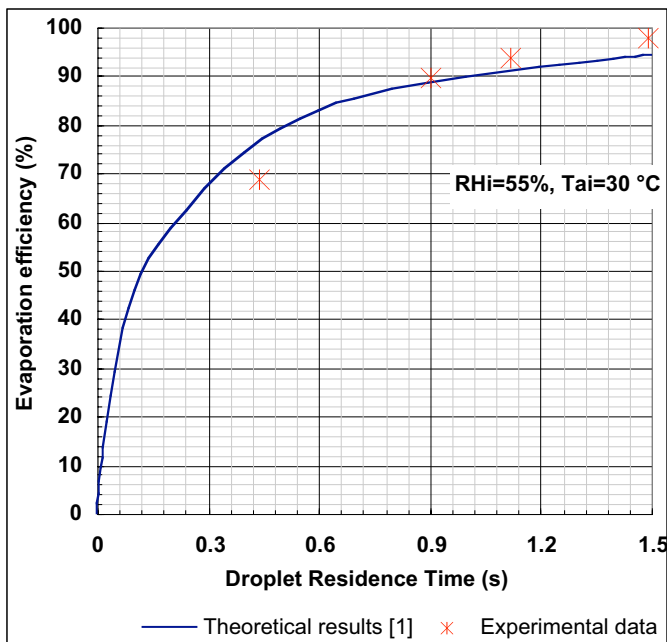


Figure 23. Correlation between theoretical model prediction and experimental data

8. CLOSURE

This paper has provided the results of extensive experimental and theoretical studies conducted on impaction pin fog nozzles used for gas turbine inlet air fogging and the dynamics of inlet fogging in

general. It has been shown that inlet fogging nozzles produce smaller droplets at higher airflow velocities but that ambient humidity levels do not significantly affect droplet size, when measurements are taken within about 20 cm (7.9") of the orifice. Droplet size tests were performed on nozzle with intentionally dislocated impaction pins and it is shown that, unless gross impaction pin dislocations are made, the droplet size remains essentially the same. The phenomenon of large droplet generation (sprinkle) from both impaction pin and swirl jet nozzles has been examined and in has been shown that, for the Mee impaction pin nozzle, sprinkle goes away at the higher operating pressures and does not significantly impact fog system performance or operational safety. An improved numerical model for predicting fog evaporation rates is presented along with discussion and curves for different initial conditions. The curves make it possible to quantitatively analyze different fog sprays under various ambient climate conditions. The given data are applied to a discussion of the ideal location of fog nozzles in the gas turbine intake air duct and the effect that a particular location will have on the evaporative efficiency of the fog system, as well as the droplet size of fog that may enter the compressor. Experimental results for evaporation time were found to be compatible, within the range of experimental uncertainty, with the predictions obtained by the numerical model.

REFERENCES

- [1] Chaker, M., Meher-Homji, C.B., Mee T.R. III, (2002) "Inlet Fogging of Gas Turbine Engines-Part A: Fog Droplet Thermodynamics, Heat Transfer and Practical Considerations," Proceedings of ASME Turbo Expo 2002, Amsterdam, The Netherlands, June 3-6, 2002, ASME Paper No: 2002-GT-30562.
- [2] Chaker, M., Meher-Homji, C.B., Mee T.R. III, (2002) "Inlet Fogging of Gas Turbine Engines-Part B: Fog Droplet Sizing Analysis, Nozzle Types, Measurement and Testing," Proceedings of ASME Turbo Expo 2002, Amsterdam, The Netherlands, June 3-6, 2002, ASME Paper No: 2002-GT-30563.
- [3] Chaker, M., Meher-Homji, C.B., Mee T.R. III, (2002) "Inlet Fogging of Gas Turbine Engines-Part C: Fog Behavior in Inlet Ducts, CFD Analysis and Wind Tunnel Experiments," Proceedings of ASME Turbo Expo 2002, Amsterdam, The Netherlands, June 3-6, 2002, ASME Paper No: 2002-GT-30564.
- [4] Meher-Homji, C.B., Mee, T.R., (1999) "Gas Turbine Power Augmentation by Fogging of Inlet Air," Proceedings of the 28th Turbomachinery Symposium, Houston, TX, September 1999.
- [5] Meher-Homji, C.B., and Mee, T.R. (2000) "Inlet Fogging of Gas Turbine Engines-Part A: Theory, Psychrometrics and Fog Generation and Part B: Practical Considerations, Control and O&M Aspects," ASME Turbo Expo 2000, Munich May 2000. ASME Paper Nos: 2000-GT-0307 and 2000-GT-0308
- [6] Kleinschmidt, R.V., (1946) "The Value of Wet Compression in Gas Turbine Cycles," Annual Meeting of the ASME December 2-6, 1946.
- [7] Wilcox, E.C., and Trout, A.M., (1951) "Analysis of Thrust Augmentation of Turbojet Engines by Water Injection at the Compressor Inlet Including Charts for Calculation Compression Processes with Water Injection," NACA Report No: 1006.

- [8] Hill, P.G. (1963), “*Aerodynamic and Thermodynamic Effects of Coolant Ingestion on Axial Flow Compressors.*” Aeronautical Quarterly, February 1963, pp 333-348.
- [9] Arsen’ev, L.V. and Berkovich, A.L. (1996) “*The Parameters of Gas Turbine Units with Water Injected into the Compressor.*” Thermal Engineering, Vol. 43, No 6, 1966, pp 461-465.
- [10] Nolan, J.P. and Twombly, V.J., (1990), “*Gas Turbine Performance Improvement Direct Mixing Evaporative Cooling System.*” ASME Paper No: 90-GT-368, International Gas Turbine and Aeroengine Congress, Brussels, Belgium, June 11-14, 1990.
- [11] Utamura, M., Kuwahara, T., Murata, H. Horii, N., (1999) “*Effects of Intensive Evaporative Cooling on Performance Characteristics of Land-Based Gas Turbine.*” Proceedings of the ASME International Joint Power Generation Conference, 1999.
- [12] Le Coz J.F, (1998) “*Comparison Of Different Drop Sizing Techniques On Direct Injection Gasoline Sprays.*” 9th International Symposium On Application Of Laser Techniques To Fluid Mechanics, Lisbon 13-16 July 1998.
- [13] Hinze, J.O., “*Fundamentals of the Hydrodynamic Mechanism of Splitting in Dispersion Process.*” AICHE J., Vol. 1, No. 3, 1955, pp. 289-295
- [14] York, J.L., Stubbs, H.F., Tek, M.R., “*The mechanism of Disintegration of Liquid Sheets.*” Trans. ASME, vol. 75, 1953, pp. 1279- 286
- [15] Chaker, M., Meher-Homji, C.B., Mee T, Nicolson, A., (2001) “*Inlet Fogging of Gas Turbine Engines- Detailed Climatic Analysis of Gas Turbine Evaporative Cooling Potential in the USA.*” ASME International Gas Turbine and Aeroengine Conference, New Orleans, USA, June 4-7, 2001, ASME Paper No. 2001-GT-526. Also to appear in ASME Transactions of Gas Turbine and Power.
- [16] Chaker, M., Meher-Homji, C.B., (2002) “*Inlet Fogging of Gas Turbine Engines- Detailed Climatic Analysis of Gas Turbine Evaporative Cooling Potential for International Locations.*” presented at ASME Turbo Expo 2002, Amsterdam, June 3-6, 2002, ASME Paper No: 2002-GT-30559.
- [17] Hoffmann, J, “*Inlet Air Cooling Performance and Operation*”, P.P. 222-227, T1-A-39, CEPSI 2002, Fukuoka, Japan.

ANNEX 1

Definitions of droplet diameters used in gas turbine inlet fogging applications and some parameters used in the paper:

Dv90 is a diameter for which 90% of the water volume in the spray is less than or equal to. A small value of this number indicates that a very small number of larger droplets are present. A small Dv90 minimizes the potential for impaction on obstructions and droplet fallout due to

gravity (both of which reduce water pooling on the duct floor) and reduces the potential for compressor blade distress.

Sauter Mean Diameter (SMD or D32) is the diameter of a hypothetical droplet whose ratio of volume to surface area is equal to that of the entire spray. Since it deals with surface area, Sauter mean diameter is a good way to describe a spray that is used for processes involving evaporation. To enhance droplet evaporation one has to maximize the active surface area and minimize the internal volume of the droplet, thus the lower the Sauter Mean Diameter, the more rapid the evaporation process.

Evaporation efficiency: This is the percent of quantity of water evaporated compared to the total quantity of injected water.

Cumulative volume frequency of droplets: This is the total volume of spray contained in droplets below a given diameter.

Active Radius RA: is the volume around the droplet for which saturation conditions are calculated